International Journal of Thermophysics, Vol. 22, No. 1, 2001

Critical Frequency Dependence of the Shear Viscosity[1]

G. Flossmann,[2] R. Folk,[2,3] and G. Moser[4]

Recent low-gravity measurements of the shear viscosity in xenon near its critical point are compared with theoretical results obtained within the field theoretical renormalization group (RG) theory. Nonasymptotic effects and gravity effects are included in our theoretical description, which allows a comparison outside the asymptotic region as well as with earthbound experiments affected by gravity. Comparisons are also made with the theoretical result of the mode coupling theory. In both theories no agreement with the frequency dependence of the real part of the shear viscosity within one-loop theory can be reached. The experimental value of the ratio of the imaginary part to the real part of the shear viscosity at T_c is found to be in agreement with the value calculated within the decoupled mode theory using the two-loop value for the critical exponent of the temperature dependence of the shear viscosity, but not with the one-loop value obtained in RG theory. Thus a complete two-loop calculation of the vertex function for the shear viscosity is required.

KEY WORDS: critical point; dynamic critical phenomena; renormalization group theory; shear viscosity; transport coefficients; xenon.

1. INTRODUCTION

Close to the critical point of a liquid–gas phase transition, the shear viscosity $\bar{\eta}$ is expected to show some interesting behavior. Exactly at the critical point (for $T = T_c$ and $\rho = \rho_c$), the shear viscosity diverges and shows a characteristic power-law behavior (e.g., $\bar{\eta} \propto |T - T_c|^{-\nu x_\eta}$ at $\rho = \rho_c$) in the asymptotic region. Farther away, we find a crossover from the

[1] Paper presented at the Fourteenth Symposium on Thermophysical Properties, June 25–30, 2000, Boulder, Colorado, U.S.A.

[2] Institute for Theoretical Physics, Johannes-Kepler-University Linz, Altenbergerstr. 69, A-4040 Linz, Austria.

[3] To whom correspondence should be addressed.

[4] Institute for Physics and Biophysics, Paris-London-University Salzburg, Hellbrunnerstr. 34, A-5020 Salzburg, Austria.

asymptotic behavior to the analytic background behavior in temperature as well as in density.

However, the experiments show a finite shear viscosity even very near the critical point. The first reason for the observed finite value of $\bar{\eta}$ at the critical point is that the shear viscosity depends on the frequency in the critical region and remains finite at nonzero frequency so that its asymptotic behavior can be seen only for vanishing frequencies. The second reason for the absence of a diverging shear viscosity in earthbound experiments is that gravity induces a density gradient in the liquid which causes the average shear viscosity to approach a finite value at the critical point.

In Refs. 1 and 2 we have calculated a theoretical expression for the shear viscosity which can be used to describe the asymptotic behavior of $\bar{\eta}$ as well as the crossover to the background behavior while considering frequency and gravitational effects. In Refs. 2 and 3 we compared the theory to earthbound experiments as well as to recent microgravity experiments onboard a space shuttle [4], which allowed for the first time experimental verification of the so far only theoretically predicted frequency effects.

2. THE DYNAMIC MODEL

As shown in Ref. 1 the shear viscosity is determined by the dynamic correlation function of the transverse momentum density $\mathbf{j}_t$ in the limit $k \to 0$ and can be described within the model H [5]. The model H contains dynamic equations for the order parameter ϕ_0 (the entropy density) and the transverse momentum density,

$$\frac{\partial \phi_0}{\partial t} = \mathring{\Gamma} \nabla^2 \frac{\delta H}{\delta \phi_0} - \mathring{g} (\nabla \phi_0) \frac{\delta H}{\delta \mathbf{j}_l} + \Theta_\phi \tag{1}$$

$$\frac{\partial \mathbf{j}_t}{\partial t} = \mathring{\lambda}_t \nabla^2 \frac{\delta H}{\delta \mathbf{j}_t} + \mathring{g} \mathscr{T} \left\{ (\nabla \phi_0) \frac{\delta H}{\delta \phi_0} - \sum_k \left[j_k \nabla \frac{\delta H}{\delta j_k} - \nabla_k \mathbf{j} \frac{\delta H}{\delta j_k} \right] \right\} + \mathbf{\Theta}_t \tag{2}$$

with fast fluctuating forces Θ_i and the projector $\mathscr{T}$ to the direction of the transverse momentum density. The Hamiltonian appearing in the dynamic equations is the normal Hamiltonian of a ϕ^4-theory together with the conserved density $\mathbf{j}_t$ entering quadratically:

$$H = \int d^d x \left\{ \frac{1}{2} \mathring{r} \phi_0^2 + \frac{1}{2} (\nabla \phi_0)^2 + \frac{\mathring{u}}{4!} \phi_0^4 + \frac{1}{2} a_j \mathbf{j}_t^2 \right\} \tag{3}$$

As described in Ref. 1 the dynamic equations may be transformed into a dynamic functional leading to dynamic vertex functions which can then be calculated in perturbation theory. The singularities in the vertex functions may be absorbed into Z-factors using field theoretical renormalization group theory. From these Z-factors one obtains the RG-functions determining the flow of the couplings and finally the expressions for the critical exponents.

From the vertex functions one obtains, apart from the shear viscosity, also other dynamical quantities, e.g., the characteristic frequency or the thermal diffusivity reviewed in Ref. 6.

3. THE SHEAR VISCOSITY

In Ref. 2 we have already discussed the frequency-dependent shear viscosity, but as there were no experimental data available at the time of publication, we had to constrain ourselves to a comparison of the frequency independent shear viscosity with experiments in ^{3}He, ^{4}He, CO_2, and C_2H_6. The situation has changed since, and the recent microgravity experiments of Berg et al. [4] allow a detailed analysis of frequency effects.

In Ref. 2 we have discussed the theoretical expression for the frequency-dependent shear viscosity, which is given by

$$\bar{\eta}(t, \Delta\rho, \omega) = \frac{k_B T}{4\pi} \frac{\xi_0}{\ell f_t^2(\ell)\, \Gamma(\ell)} \left[1 + E_t(f_t(\ell), v(\ell), w(\ell))\right] \tag{4}$$

with the one-loop perturbational contribution

$$\begin{aligned}
&E_t(f_t(\ell), v(\ell), w(\ell)) \\
&\quad = -\frac{f_t^2}{96} \left\{ 1 + 6 \left[i \frac{v^2}{w} \ln v + \frac{1}{v_+ - v_-} \left(\frac{v_-^2}{v_+} \ln v_- - \frac{v_+^2}{v_-} \ln v_+ \right) \right] \right. \\
&\qquad - \frac{4}{(v_+ - v_-)^3} \left[\frac{v_+^3 - v_-^3}{3} + \frac{3}{2} (v_+ - v_-)(v_+^2 \ln v_+ + v_-^2 \ln v_-) \right. \\
&\qquad \left. - (v_+^3 \ln v_+ - v_-^3 \ln v_-) \right] \\
&\qquad + \frac{2}{(v_+ - v_-)^2} \left[\frac{v_+^3}{v_-} (1 + 4 \ln v_+) + \frac{v_-^3}{v_+} (1 + 4 \ln v_-) \right. \\
&\qquad + \left(\frac{1}{v_-} - \frac{2}{v_+ - v_-} \right) \frac{v_+^4 \ln v_+ - v^4 \ln v}{v_-} \\
&\qquad \left. \left. + \left(\frac{1}{v_+} + \frac{2}{v_+ - v_-} \right) \frac{v_-^4 \ln v_- - v^4 \ln v}{v_+} \right] \right\}
\end{aligned} \tag{5}$$

The parameters introduced in Eq. (5) are defined as

$$v(\ell)=\frac{\xi^{-2}(t)}{(\xi_0^{-1}\ell)^2},\qquad w(\ell,\omega)=\frac{\omega}{2\Gamma(\ell)(\xi_0^{-1}\ell)^4},\qquad v_\pm(\ell,\omega)=\frac{v}{2}\pm\sqrt{\left(\frac{v}{2}\right)^2+iw} \tag{6}$$

The crossover from the asymptotic to the background behavior is governed by the mode coupling $f_t(\ell)$ and the Onsager coefficient $\Gamma(\ell)$, which are given by

$$f_t(\ell)=\frac{24}{19}\left[1+\frac{\ell}{\ell_0}\left(\frac{24}{19f_0^2}-1\right)\right]^{-1} \tag{7}$$

$$\Gamma(\ell)=\Gamma_0\left(\frac{19f_0^2}{24}\frac{\ell_0}{\ell}\left[1+\frac{\ell}{\ell_0}\left(\frac{24}{19f_0^2}-1\right)\right]\right)^{1-x_\eta} \tag{8}$$

where Γ_0, f_0, and ℓ_0 are the initial values of the Onsager coefficient Γ, the mode coupling f_t, and the flow parameter ℓ, all determined at a fixed temperature $t=t_0$ at the critical isochore.

In Eq. (8) we have inserted the critical exponent $1-x_\eta$ instead of its one-loop value 18/19, as we treat the exponent x_η as an additional free parameter which will be fitted from the experimental data. The reason for using other than the one-loop value $x_\eta=0.054$ is that it is far away from the guessed value $x_\eta\approx 0.065$ from experimental analysis and, therefore, not suitable for comparison with experiments. Even the theoretical values for this exponent differ in the literature depending on the method of calculation used (see Ref. 2 for a listing).

The flow parameter ℓ is responsible for the crossover from the asymptotics (for $\ell\to 0$) to the background (for $\ell\to\infty$) and connected to the correlation length ξ and the frequency ω via the matching condition (which appears naturally within the calculation setting certain logarithmic terms in the vertex functions to zero)

$$\left(\frac{\xi_0}{\xi}\right)^8+\left(\frac{2\omega}{\Gamma(\ell)}\right)^2=\ell^8 \tag{9}$$

where ξ_0 is the amplitude of the correlation length. The initial value ℓ_0 of the flow parameter is found from Eq. (9) at zero frequency inserting the value $\xi(t_0)$ of the correlation length evaluated at t_0 and ρ_c.

The correlation length itself is a function of temperature and density and may be found using the restricted cubic model [7] discussed in Ref. 2, where the reduced temperature t and the reduced density $\Delta\rho$ are expressed in terms of new variables r and θ,

$$t = \frac{T - T_c}{T_c} = (1 - b^2\theta^2)\, r, \qquad \Delta\rho = \frac{\rho - \rho_c}{\rho_c} = k(\theta + c\theta^3)\, r^\beta \tag{10}$$

The correlation length ξ is given by the heuristic expression

$$\xi = \xi_0(1 + 0.16\theta^2)\, r^{-\nu} = \xi_0 t^{-\nu}(1 + 0.16\theta^2)(1 - b^2\theta^2)^\nu \tag{11}$$

so that Eq. (10) can be inverted numerically to get the correlation length as a function of the reduced temperature and the reduced density. Inserting $\xi(t, \Delta\rho)$ into the matching condition, Eq. (9), and the corresponding flow parameter $\ell(t, \Delta\rho, \omega)$ into Eqs. (4)–(8), we get the shear viscosity as a function of temperature, density, and frequency. We also should note that Eq. (5) simplifies significantly at zero frequency and is given in Ref. 2.

In Fig. 1 we show the shear viscosity along the critical isochore as a function of the reduced temperature for various values of the frequency. We see that in the absence of gravitation the shear viscosity follows the asymptotic power law $\bar{\eta} \propto \xi^{x_\eta} \propto t^{-\nu x_\eta}$ at zero frequency for small values of the reduced temperature, whereas for nonzero frequencies it approaches a finite value at T_c. If gravitation is included, however, the frequency effects are masked by gravitational effects (except for very large frequencies) so that frequency effects are visible only in microgravity experiments. As discussed in Ref. 2 the reason is that in nonzero gravity we find a density gradient in the liquid leading to a dependence of the correlation length and thus of the shear viscosity on the vertical position in the vessel. Now the shear viscosity is usually measured in a vessel with two rotating disks at the bottom and the top so that the gravity average of the shear viscosity $\bar{\eta}_{av}$ consists simply of the contributions of the viscosity or, more precisely, the decrement $D \propto \sqrt{\eta\rho}$ at the bottom and the top,

$$\bar{\eta}_{av}(t) = \frac{(\sqrt{\bar{\eta}_b \rho_b} + \sqrt{\bar{\eta}_t \rho_t})^2}{4\rho_c} \tag{12}$$

The limiting value of the average shear viscosity depends basically on the initial value of the mode coupling f_0 and the critical exponent x_η which might allow an exact determination of x_η.

4. COMPARISON WITH EXPERIMENTS

In this section we compare our theoretical expression for the frequency-dependent shear viscosity with the microgravity data of Berg et al.

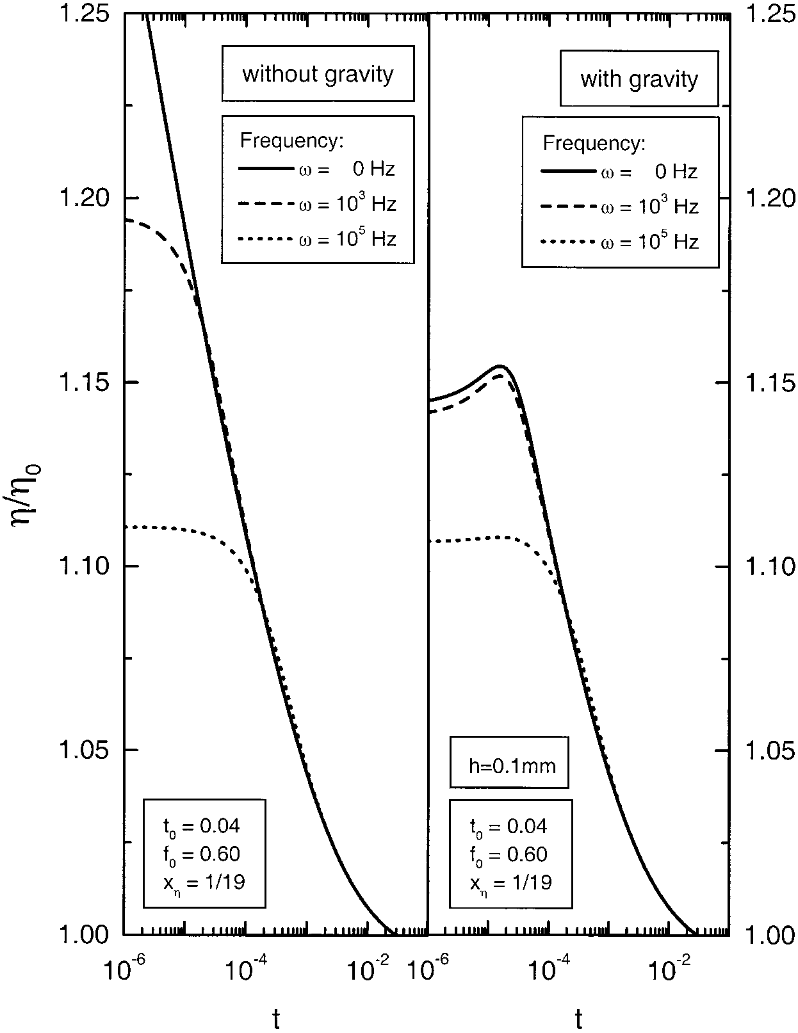

Fig. 1. The frequency-dependent shear viscosity (with $x_\eta = 1/19$) with and without gravitation for various frequencies.

[4] for Xe. They not only measured the real part of the shear viscosity but also determined the imaginary part from the phase shift so that we are able to compare our theoretical results for $\mathrm{Re}(\bar{\eta})$ as well as for the ratio $\mathrm{Im}(\bar{\eta})/\mathrm{Re}(\bar{\eta})$ with these experiments as shown in Figs. 2 and 3.

Berg et al. compared their experimental results with the mode coupling theory of Bhattacharjee et al. [8] and found that they could describe their

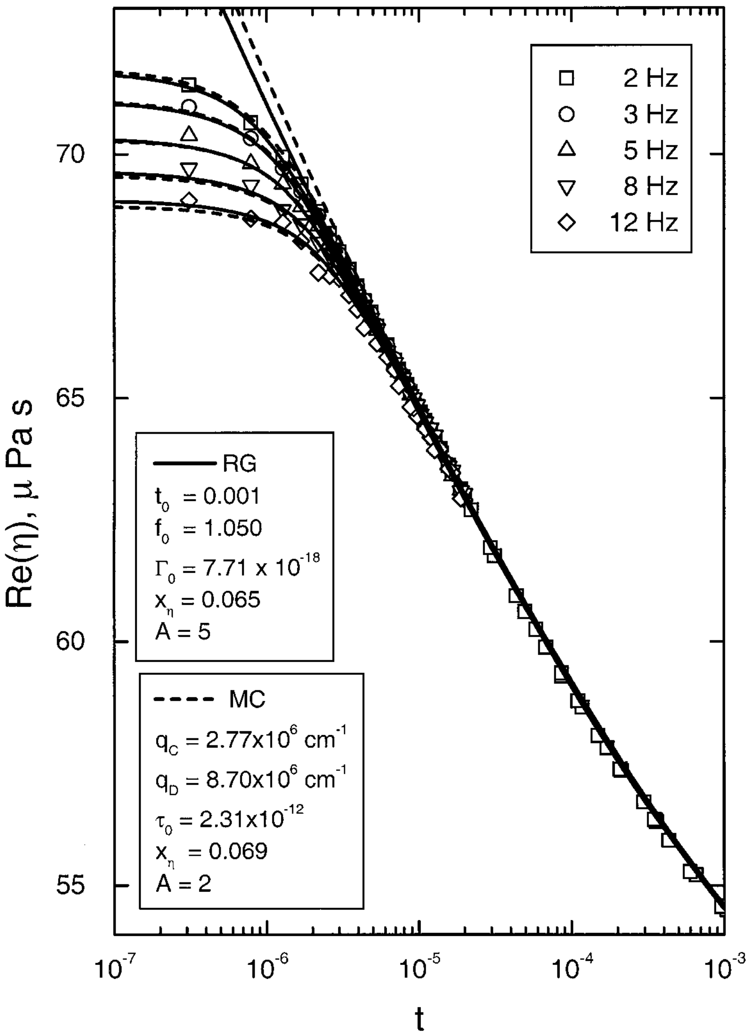

Fig. 2. Comparison of the real part of the frequency-dependent shear viscosity evaluated in renormalization group theory with $x_\eta = 0.065$ (solid curves) and mode coupling theory with $x_\eta = 0.069$ (dashed curves) with experiments in microgravity [4]. In renormalization group theory the frequency was multiplied by a factor $A = 5$, and in mode coupling theory by $A = 2$ (see text for explanation).

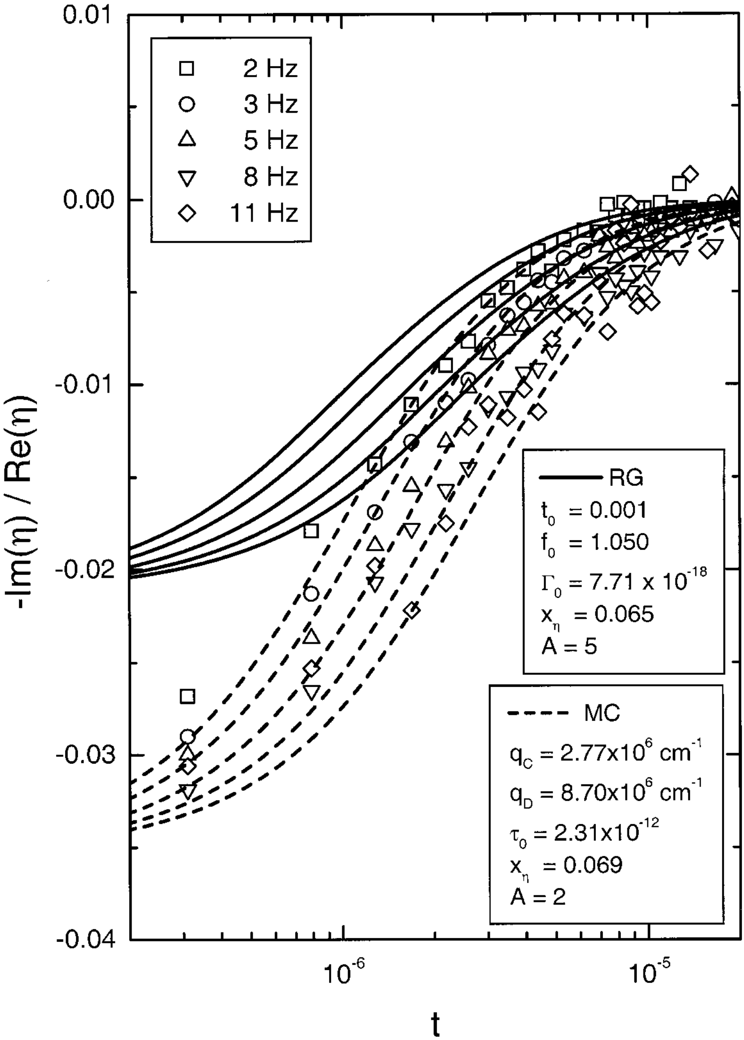

Fig. 3. Comparison of the ratio $\mathrm{Im}(\bar{\eta})/\mathrm{Re}(\bar{\eta})$ of the frequency-dependent shear viscosity evaluated in renormalization group theory with $x_\eta = 0.065$ (solid curves) and mode coupling theory with $x_\eta = 0.069$ (dashed curves) with experiments in microgravity [4]. In renormalization group theory the frequency was multiplied by a factor $A = 5$, and in mode coupling theory by $A = 2$ (see text for explanation).

data correctly only by multiplying the frequency by a factor of 2 in the theoretical expressions. They explained the introduction of this factor as a two-loop effect correcting the errors of the one-loop expression used for the frequency-dependent shear viscosity. As discussed in Ref. 3 we reach practically the same quality of agreement for $\mathrm{Re}(\bar{\eta})$ with our theory if we multiply the frequency by a factor of 5, which may be justified for the same reason as the factor of 2 in the mode coupling theory. Of course, the experimental data of the earthbound experiments in Xe are well described without this factor since, from the discussion above, frequency effects play no role [3].

In Fig. 2 we compare our renormalization group result for $\mathrm{Re}(\bar{\eta})$ as well as the corresponding mode coupling expression [8] with the experimental data (all parameters are indicated in the plot) and find good agreement for both theories. However, both theories fail to describe the experimental data correctly if no multiplicative factor for the frequency is used.

As already mentioned we have treated the critical exponent as an additional fit parameter in our theory. Therefore, we started with the shear viscosity data and chose t_0 to determine the initial value of the Onsager coefficient Γ_0 as a function of the initial value of the mode coupling f_0 from the value of $\bar{\eta}(t_0)$. Then, we used the experimental data for the characteristic frequency in Xe (see Ref. 6) to fit f_0 in the nonasymptotic region with x_η kept at its one-loop value, 1/19. With $\Gamma_0(f_0)$ and the set of parameters t_0 and f_0, we returned to the data for the shear viscosity and, finally, fitted the exponent x_η in the asymptotic region (see Refs. 2 and 3 for details). This procedure yielded the value $x_\eta = 0.065$ instead of the $x_\eta = 0.069$ used by Berg et al. We should note here that we can also use the exponent $x_\eta = 0.069$ (with different initial values for f_0 and Γ_0) to get exactly the same quality of agreement as shown in Ref. 9 but then we are not able to describe the characteristic frequency data correctly with this choice of f_0 and Γ_0.

In the way described above, the specific flow of the mode coupling f_t for xenon is fixed. No further free parameter remains for the shear viscosity at finite frequencies or other dynamical quantities. The appropriate coupling as a function of temperature t and frequency ω is shown in Fig. 4 together with the range of the experiments in xenon (dark area). The experimental data lie on the plateau of the fixed point value as well as on the slope of the crossover to the background value.

Applying the mode coupling theory (with an exponent $x_\eta = 0.069$), Berg et al. also found good agreement for the ratio $\mathrm{Im}(\bar{\eta})/\mathrm{Re}(\bar{\eta})$. Comparing our results with these experimental data, we get less satisfactory results [9] because in our theory the ratio $\mathrm{Im}(\bar{\eta})/\mathrm{Re}(\bar{\eta})$ approaches the finite value

$$\lim_{T\to T_c} \frac{\mathrm{Im}(\bar{\eta})}{\mathrm{Re}(\bar{\eta})} = \frac{1}{76}\,\frac{\pi}{2}\left[1 - \frac{1}{76}\{3\ln(1/4) - 1/3\}\right]^{-1} \approx 0.0195 \tag{13}$$

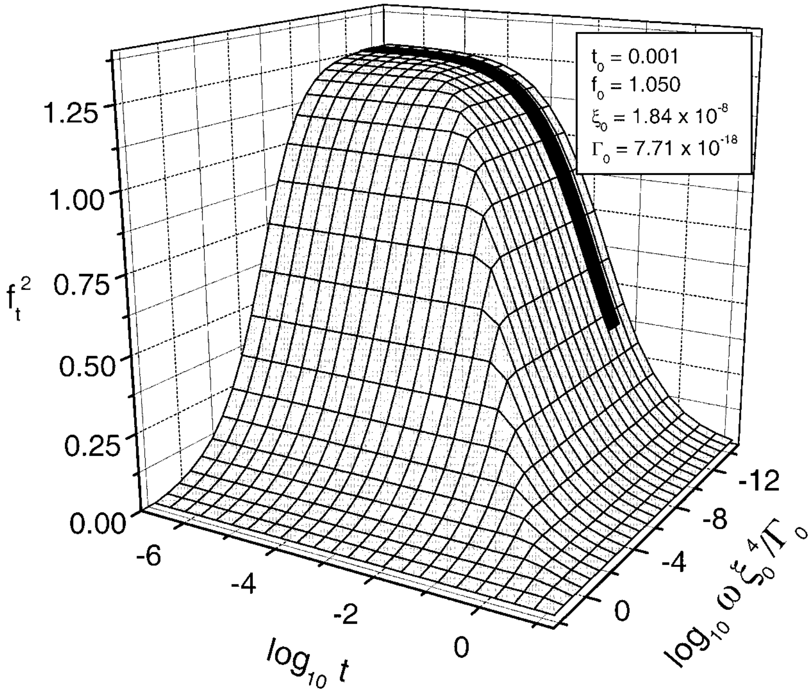

Fig. 4. Mode coupling $f_t^2(t, \omega)$ (all nonuniversal parameters for xenon) as a function of the reduced temperature t and the dimensionless frequency $\omega/\Gamma_0\xi_0^{-4}$ along the critical isochore. For small values of the frequency and reduced temperature we reach the fixed point value $f_t^{*2} = 24/19$. The dark region marks the range of experimental shear viscosity data for xenon.

at T_c, which is different from the value 0.0353 obtained from the mode coupling theory with the exponent $x_\eta = 0.069$ [4]. As the limit of the ratio $\mathrm{Im}(\bar{\eta})/\mathrm{Re}(\bar{\eta})$ does not contain any free parameter at T_c, it cannot be improved other than by going to higher-loop orders. This is shown in Fig. 3 where we compare our theory and the mode coupling theory with the experimental data. In this respect we should also note that the mode coupling expression used by Berg et al. is not purely of one-loop order since it makes use of the experimental value for the exponent x_η, which differs significantly from its one-loop value. If we insert the one-loop value $x_\eta = 1/19$ into the mode coupling expressions, we would get a limit $\mathrm{Im}(\bar{\eta})/\mathrm{Re}(\bar{\eta}) \approx 0.0271$ at T_c, which is also significantly lower than the measured limiting ratio. So a major difference between the mode coupling theory and our theory is that it is not possible to introduce the true critical exponent x_η in our expression for $\mathrm{Im}(\bar{\eta})/\mathrm{Re}(\bar{\eta})$, and therefore, deviations from the one-loop order perturbation theory cannot be weakened by the use of the correct value for x_η.

5. CONCLUSION

We have seen that we can describe the microgravity data for the real part of the shear viscosity very well with our theory if we introduce a multiplicative factor for the frequency which may be interpreted as a correction coming from higher-order perturbation contributions. Then we can also describe earthbound shear viscosity experiments [3] as well as light scattering experiments [3, 6] in Xe with the same set of parameters. However, our one-loop theory fails to describe the experimental data for the ratio $\mathrm{Im}(\bar{\eta})/\mathrm{Re}(\bar{\eta})$ correctly and we may expect improvements from a two-loop theory currently in progress.

ACKNOWLEDGMENT

This work was supported by the Fonds zur Förderung der wissenschaftlichen Forschung under Project No. P12422-TPH.

REFERENCES

1. R. Folk and G. Moser, *Phys. Rev. E* **57**:683 (1998); *Phys. Rev. E* **57**:705 (1998).
2. G. Flossmann, R. Folk, and G. Moser, *Phys. Rev. E* **60**:779 (1999).
3. G. Flossmann and R. Folk, *Phys. Rev. E* **62**:2460 (2000).
4. R. F. Berg, M. R. Moldover, and G. A. Zimmerli, *Phys. Rev. Lett.* **82**:920 (1999); *Phys. Rev. E* **60**:4079 (1999).
5. P. C. Hohenberg and B. I. Halperin, *Rev. Mod. Phys.* **46**:435 (1977).
6. G. Flossmann and R. Folk, submitted for publication.
7. C.-C. Huang and J. T. Ho, *Phys. Rev. A* **7**:1304 (1973).
8. J. K. Bhattacharjee, R. A. Ferrell, R. S. Basu, and J. V. Sengers, *Phys. Rev. A* **24**:1469 (1981); J. K. Bhattacharjee and R. A. Ferrell, *Phys. Rev. A* **27**:1544 (1983).
9. R. Folk, *Condensed Matter Phys. (Ukraine)* **2**:359 (2000).